Challenges of cathodic protection in high-performance concrete: The impact of electrical resistivity

Shamir Bhuiyan[1], and *David* Law[1]

[1] RMIT University, Melbourne, VIC, 3001, Australia

Abstract: Utilization of high-performance concrete (HPC) incorporating supplementary cementitious materials (SCMs), such as fly ash and slag, is becoming increasingly popular in modern construction. While such concrete can have desirable properties such as high strengths and enhanced durability, their inherently high electrical resistivities can pose a challenge should future electrochemical treatments like cathodic protection (CP) be required. To investigate the effects of high resistivities, an experiment was undertaken where steel reinforced concrete prisms were prepared using 65% cement-replacement using ground granulated blast furnace slag (GGBS) and 30% Class F Fly Ash and were periodically subject to short term CP as the concrete dried. The test involved periodic resistivity measurements and short-term CP application while monitoring polarization of the steel bar with respect to embedded reference electrodes. The output voltage required to operate the CP in galvanostatic mode was also monitored. The results demonstrated that the resistivity of the slag specimen reached a point beyond which the power supply's output capacity was reached. Moreover, the current distribution was observed to become less uniform as resistivity increased. This paper highlights an often-overlooked aspect of high-performance concrete incorporating SCMs, emphasizing the hypothetical yet important limitations that may arise for future electrochemical treatments if required.

1 Introduction

In the last two decades, the use of high-performance concrete (HPC) and ultra high-performance concrete (UHPC) has gained significant popularity in the construction industry due to their exceptional strengths, durability characteristics, and enhanced long-term performances.

HPC derives its exceptional characteristics from engineered mix designs that incorporate supplementary cementitious materials (SCMs) such as fly ash, silica fume, or slag alongside advanced chemical additives like superplasticizers which enable the formulation of concrete with exceptionally low water-to-cement ratios and remarkably dense microstructures. As a result, this significantly reduces the diffusion of harmful species into the concrete, thereby increasing resistance to degradation. Studies have shown that chloride diffusion coefficients of HPC and UHPC are between one and three orders of magnitude lower than that of 'normal strength concrete' [1]. Moreover, corrosion of reinforcing bars is significantly impeded as ionic current flow cannot occur easily between anodic and cathodic areas due to the inherently high electrical resistivities. A study on UHPCs revealed that these materials typically exhibit resistivity values exceeding 1000 Ω·m [2]. Additionally, when immersed in chloride solutions, they displayed negligible corrosion current densities (< 0.025 μA/cm²) even after nearly one year of testing—almost an order of magnitude lower than that observed in a conventional 50 MPa concrete mix.

While the high resistivities of HPCs (and UHPCs) mean that they are less prone to corrosion in the early stages of their service life, any subsequent degradation—whether due to long-term progressive corrosion, construction defects, loading conditions, or special cases where corrosion is accelerated—raises concerns regarding the effectiveness of application of electrochemical rehabilitation techniques such as cathodic protection (CP). For decades, CP has been effectively used to control corrosion of steel reinforcement in conventional concrete [3-5], however with the rise in use of HPCs in construction, the question of how effectively CP can perform in mitigating corrosion (if and when required) becomes particularly pertinent. The question is largely hypothetical at present, because construction using HPCs is relatively recent and significant corrosion problems are not expected to surface for many years. Nevertheless, it is highly likely that at some point in their service, life HPC's will present reinforcement corrosion.

1.1 Effect of Electrical Resistivity on ICCP

Electrical resistivity plays a crucial role in the performance of an ICCP system, as it strongly impacts current distribution to the steel reinforcement. Research indicates that higher concrete resistivity leads to poorer current distribution, with steel closest to the anode receiving a disproportionately larger share of the applied current. In studies conducted on samples with multiple layers of reinforcement, the steel layer closest to the anode was observed to receive significantly more

current than those further away. These were generally in the range 70-90% of the total current, though shielding effects due to the reinforcement orientation were also postulated as a factor influencing current distribution [6-8].

Moreover, higher concrete resistivity has been shown to result in a lower throw of current [6-9]. In accordance with Ohm's law, a path of greater resistance will result in a lower current for a given driving voltage, resulting in lower polarization. Consequently, the quantity of current, and hence the level of protection received is dependent on the position of the bars in relation to the anode and the resistivity of the concrete.

Studies have shown that in low-resistivity concrete, current distribution is primarily governed by polarization behaviour, whereas in high-resistivity concrete, resistivity itself becomes the dominant factor [10]. Polarization behaviour is influenced by corrosion activity, with lower corrosion rates resulting in a more uniform current distribution [7]. Consequently, for high-resistivity concrete such as HPCs and UHPCs, where corrosion rates are generally very low, the uniformity of current distribution is expected to be better, noting that this is the case when the corrosion rate does not vary over the steel surface [6,7]. However, if cracking has occurred then this would influence the current distribution.

Thus, when considering the application of CP on structures with HPC, consideration of the influence of resistivity on the current distribution and the impacts on the protection afforded to the steel is critical. To address this issue, in this study the impact of resistivity on CP application is examined using laboratory-prepared concrete specimens incorporating supplementary cementitious materials (SCM) to produce concrete specimens with a range of resistivities. The SCM utilized are Class F Fly Ash (FA) and Ground Granulated Blastfurnace Slag (GGBS). The specimens were allowed to dry in ambient laboratory conditions and were periodically subjected to short-term (10-minute) application of ICCP to assess the effects of resistivity on the output voltage and steel potentials.

2 Methodology

Three concrete prisms, each measuring 350 x 100 x 100 mm, were cast using different mix designs: N30 (Nominal 30 MPa concrete with GP cement), FA30 (fly ash concrete with 30% cement replacement), and S65 (slag concrete with 65% slag replacement). The GP cement was Type 1 Portland cement complying with AS 3972 standard [11]. The SCM utilized were low calcium Class F fly ash, specific gravity 2.4, Eraring Power Plant and commercial grade GGBS from Independent cement. The coarse aggregate was 7 mm and 10 mm Basalt with specific gravity 2.65. The sand utilized was uncrushed river sand with a fineness modulus of 2.5 and a specific gravity of 2.5. The coarse aggregates were used in the saturated surface-dry condition while the sand was used in a fully dry condition. Tap water was used throughout. A 2% NaCl admixture was added to each mix to study corrosion effects, though this aspect is beyond the scope of this paper. The details of the concrete mixes are summarised in Table 1.

Table 1. Concrete mix details

Constituents	Quantity (Kg/m^3)		
	N30	**FA30**	**S65**
(GP) Cement	400	280	140
Fly Ash	0	120	0
Ground-granulated blast-furnace slag	0	0	260
Water (w/b: 0.55)	220	220	220
Fine Aggregate	615	615	615
Coarse Aggregate (7mm)	550	550	550
Coarse Aggregate (10mm)	550	550	550
NaCl	8	8	8

Each prism contained a single 12 mm deformed reinforcing bar, embedded along the length of the specimen. Additionally, an 80 mm MMO ribbon anode strip of 25mm width was installed at one end of the prism (top corner) with 10 mm cover. Reference electrodes were fabricated using PVC tubing plugged with a porous wooden stopper at the ends. The tubes were filled with $CuSO_4$ solution and a Cu wire inserted prior to testing to create $Cu/CuSO_4$ reference electrodes. Four reference electrodes were placed along the length of each reinforcing bar at 80 mm spacings.

The dry materials comprising the Portland cement, SCM (FA30, S65), sand, and coarse aggregate were premixed in a planetary mixer for approximately 3 minutes, until homogenised. The water was added and mixed for a further 3-5 minutes. When the mixture achieved a glossy and homogeneous appearance, it was placed into moulds in two layers and vibrated for 30 seconds on a vibrating table. The specimens were kept under ambient conditions, approx. 25 ^oC, for 24 hrs before demolding. After 24 hours the specimens were transferred to a spray chamber for curing where they were subject cyclic spraying using tap water. Spraying was conducted twice a day with 1h- spray cycles. Other short-term tests (not reported herein) were performed over the course of a year, after which the testing presented in this paper were conducted. Specimens were removed from the spray chamber and allowed to dry in ambient laboratory conditions to study the effect of progressive increase in resistivity on CP application. After 2 weeks of testing, an additional dataset was obtained following soaking specimens in a water-bath for a week to simulate saturated (or near-saturated) conditions. Periodic resistivity measurements were performed on companion cylinders cast concurrently with the prisms using a 4-point Wenner probe (Proceq Resipod) with a bulk resistivity attachment.

Following resistivity measurements, short-term impressed current cathodic protection (ICCP) was applied periodically over the drying period, using a galvanostat (ACM Field Machine), using a constant

current corresponding to a current density of 20 mA/m^2 of steel surface area. The output voltages and steel potentials (with respect to reference electrodes) were logged using a datalogger (DataTaker DT80) during CP application, which lasted 10 minutes for each test. The test setup is illustrated in Figure 1.

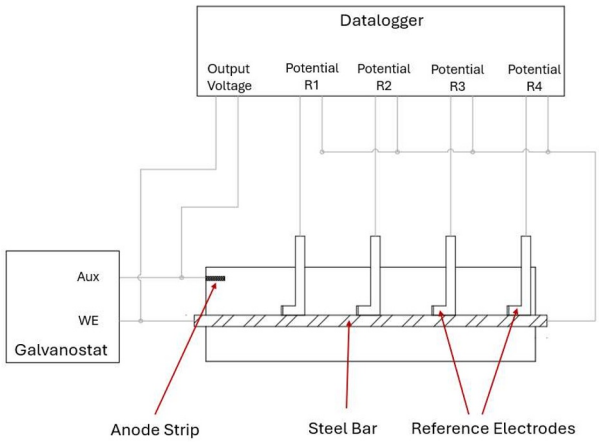

Fig. 1. Schematic of Resistivity Test Specimen

3 Results

The results are presented and discussed in the following section. These include the resistivity, output voltage and polarization.

3.1 Resistivity

The results of the development of resistivity using average resistivity data are summarised in Figure 2. Day 0 marks the first day the specimens were removed from the spray chamber. The dataset for testing after water bath soaking is positioned before day 0 on the x-axis, despite being conducted later, to maintain a logical progression in the resistivity data.

As expected, resistivity generally increases over time as the specimens dry. However, some fluctuations appear in the dataset, likely due to measurement variability or error. These inconsistencies may be caused due to wetting contact pads to ensure good contact during bulk resistivity measurements, which introduces a variable, ie, the amount of moisture present on the surface during testing. Since resistivity should progressively increase, any drops below the general trend are assumed to be measurement errors.

The results show that blended cements with fly ash and slag have significantly higher resistivities relative to the N30 mix. The FA30 was observed to have a resistivity between 2-3 times greater than the resistivity of N30, while the S65 was between 3-5 times the resistivity of N30. After 14 days of drying, the resistivity of S65 approached 1000 kΩ.cm, reaching the lower range of values typically observed for HPCs as reported in literature [1, 12].

The variation in the resistivities observed confirms that the concrete mixes designed do provide a significant difference, which becomes more pronounced as the concrete dries. This variation enables the assessment of the effect of resistivity on the application of ICCP.

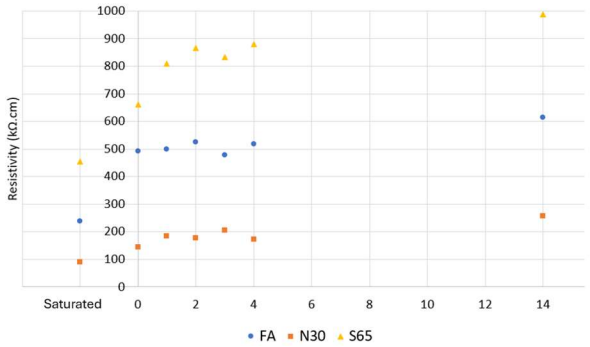

Fig. 2. Resistivity (Kohm.cm) vs Time (Days)

3.2 Output Voltage

Prior to applying CP, initial voltage readings were determined. These represent the natural potential differences that exists between the anode and the steel in concrete. Figure 3 illustrates the output voltage trends for the N30 mix, where these initial voltages can be seen in the initial period of the graph. Following the initial base readings the CP is applied for a 10-minute period. When the CP is applied, the voltage recorded is the sum of the initial voltage and the externally applied voltage of the galvanostat. During CP application, the galvanostat gradually increases the applied voltage to maintain the pre-set constant current, compensating for the rising circuit resistance over time due to effects including passive layer formation and consumption of moisture around the steel and the possible concentration polarization of the electrolyte.

In line with the increasing resistivity, due to drying, the output voltage is observed to increase at each point over the 14-day period. This increase becomes more pronounced with time. In the initial 2-day period there is little change in the resistivity compared to the saturated conditions, but by day 4 there is a clear increase and at day 14 this has become significant.

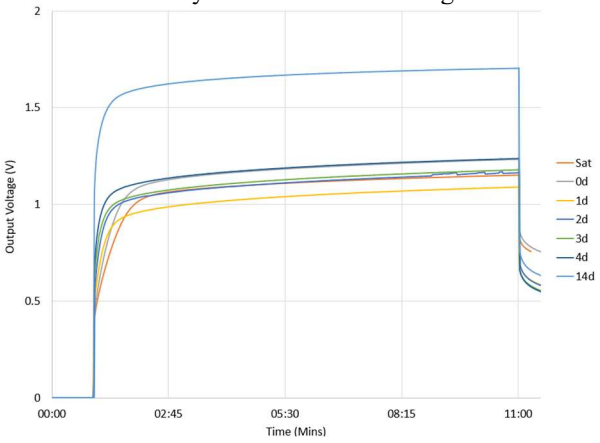

Fig. 3. Output Voltage (V) vs Time (min), N30 concrete

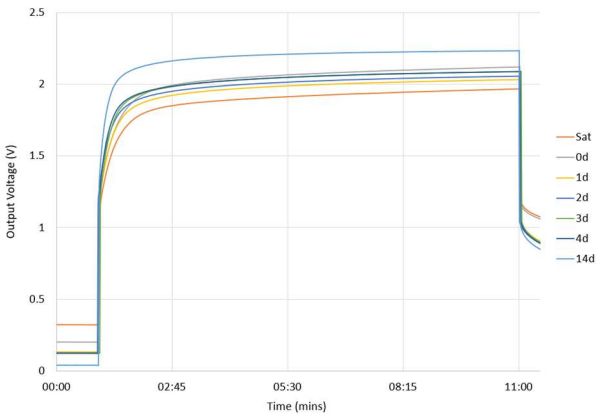

Fig. 4. Output Voltage (V) vs Time (min), FA30 concrete

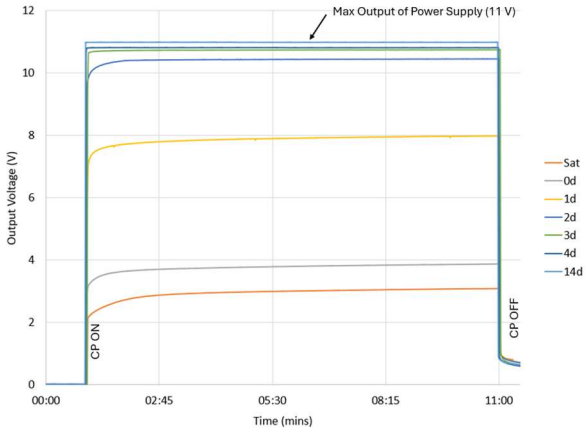

Fig. 5. Output Voltage (V) vs Time (min), S65 concrete

Figure 4 shows the output voltage verses time for FA30. For the FA30 the increase in output voltage is evident from day 0, with a steady increase in voltage evident to day 14, though the rise between day 4 and day 14 is not as pronounced as for N30.

The output voltage data for S65 is given in Figure 5. Significantly higher output voltages are required to output the same current when compared to N30 and FA30 mixes. For the 3, 4, and 14-day tests, the voltage trend takes a square form due to the maximum voltage of the galvanostat being reached due to the exceptionally high resistivity values. In these cases, the galvanostat operates in constant voltage mode at the maximum output of 11 V, which results in a progressively lower current delivery with the increase in resistance.

Table 2 summarizes the initial, minimum, and maximum recorded voltages. Notably, for N30, the maximum ON voltage at 0 and 1-day is lower than when the specimen is fully saturated, despite the higher resistivity. Similarly, for FA30, the output voltages for the day 1 to day 4 tests are lower than the maximum ON voltage at 1 day. Even after offsetting initial values, the driving volage does not show a consistent relationship with increasing resistivity, suggesting that resistivity is not the sole determining factor of output voltage. It is hypothesised that this is due to the polarization resistance of the steel which also contributes to the total circuit resistance and hence influences the output voltage. The data suggests that at lower resistivities the polarization behaviour of steel has a more significant role, however at higher resistivities, concrete resistivity becomes the dominant factor.

Table 2. Summary of output voltage measurements

Mix	Test Point/ Condition	Initial Voltage (V)	Minimum ON Voltage (V)	Maximum ON Voltage (V)
N30	Saturated	0.33	0.74	1.48
	0 d	0.20	0.62	1.43
	1 d	0.33	0.77	1.41
	2 d	0.31	0.88	1.48
	3 d	0.33	0.93	1.51
	4 d	0.33	1.00	1.57
	14 d	0.23	1.25	1.94
FA30	Saturated	0.32	1.09	1.97
	0 d	0.20	1.13	2.12
	1 d	0.13	1.13	2.03
	2 d	0.13	1.18	2.06
	3 d	0.13	1.19	2.09
	4 d	0.13	1.15	2.09
	14 d	0.03	1.26	2.23
S65	Saturated	0.44	2.54	3.51
	0 d	0.60	2.53	4.45
	1 d	0.29	6.09	8.25
	2 d	0.28	9.09	10.73
	3 d	0.25	9.44	11.00
	4 d	0.22	10.78	11.00
	14 d	0.06	11.00	11.00

Figure 6 shows the relationship between resistivity values for each of the concrete mixes and the maximum output voltages (excluding S65 values running at constant 11 V). It is observed that for the N30 and FA30 mixes, the output voltage barely increases with the increase in resistivity, however a significant increase is seen for S65. This is thought to be a function of the corrosion rates, discussed further in Section 2.3.

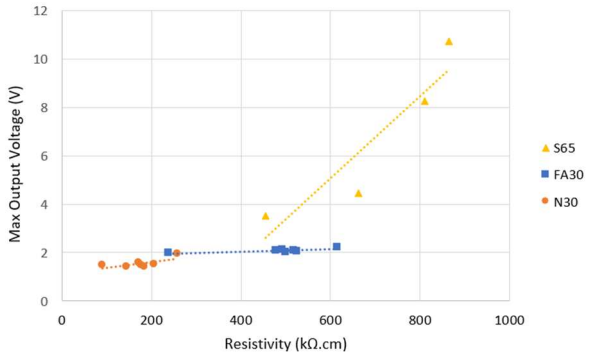

Fig. 6: Relationship between resistivity values and maximum output voltages

3.3 Polarization

Polarization is determined as the difference between the equilibrium or corrosion potential prior to the application of the CP at each time of application and the instant-off potential recorded at the end of CP application. As localised current densities on the surface of the steel cannot be practically measured, polarization is often used as an indirect basis to assess current distribution due to its direct relationship with current density. However, it should be noted that polarization data can be complicated due to its dependency on other factors such as corrosion rates.

Figure7 presents the polarization data along the length of the bar in the form of heat-maps. Results are shown for minimum and maximum resistivities (saturated and 14-day data) for each specimen, except for S65, where 2-day data is provided in lieu of 14-day. Beyond 2 days, the CP system operates in constant voltage mode, leading to variability for comparison purposes. The uniformity of polarization is also given in terms of a uniformity ratio (UR), where UR = Minimum polarization/Maximum polarization. A lower ratio indicates less uniform polarization across the bar and vice versa.

The data indicates that saturated specimens exhibit lower polarization, primarily due to the slower polarization rates caused by oxygen diffusion limitations. The polarization generally increases with time in all three mixes as the concrete dries, corresponding with the increase in resistivity in the concrete and the output voltage required to maintain the current. The highest polarization is observed in the S65 within 2 days, which is considerably higher than both N30 and FA30 at 14 days; a polarization of ~350 mV is observed in S65, and ~250 mV in FA30 and ~200 mV in N30. This shows that polarization increases with higher resistivity concrete mixes.

The data also highlights the disparity in the current distribution. The section of the bars closest to the anode experiences the greatest polarization, as expected due to receiving the largest portion of current. Over time as resistivity increases (from saturated to dry conditions), the uniformity of the current distribution becomes more even. The exception to this is S65, which shows the uniformity becoming less as the concrete dries. It is hypothesised that uniformity becomes more even for N30 and FA30 due to corrosion being inhibited with the drying of the concrete [13]. The corrosion is reduced due to less moisture remaining to drive the cathodic reaction and consequently resulting in lower corrosion rates and thus a more uniform current distribution. However, for S65, it is possible that the reduction of corrosion rates is not significant as it was likely already low initially (due to significantly higher resistivity). As a result, the effect of corrosion on uniformity is likely negligible and therefore the uniformity is mainly a function of resistivity. Thus, the uniformity is seen to decrease with increasing resistivity. Moreover, this can also be used to explain the trends observed in Figure 7. As the corrosion rates reduce for N30 and FA30, the output voltage required also reduces which counteracts the effect of increasing resistivity. However, as discussed above, S65 behaves differently as it is largely controlled by resistivity. Therefore, this highlights that current distribution, and uniformity is dependent on both concrete resistivity and corrosion rates, with concrete resistivity playing a more significant role at higher resistivities.

Furthermore, the polarization data indicates that lower resistivity concrete have better uniformity and greater throwing power, such that the steel area further from the anode receives more of the current compared to concrete with higher resistivity. This suggests that HPCs and UHPCs pose a significant challenge for CP application due to their susceptibility to uneven current distribution and reduced throwing power. As resistivity increases, the steel closest to the anode receives a disproportionately large share of the protective current, leaving more distant areas under-protected.

The high resistivities of HPCs and UHPCs will thus demand higher driving voltages to maintain the appropriate current flow to provide protection. To address these issues closer anode spacing and increased transformer rectifier capacity may be required. Hence, further increasing system complexity and power requirements to maintain the required current. Closer anode spacings translate to higher installation costs. These factors can pose significant challenges in both the design and effectiveness of CP systems in HPCs and UHPCs, requiring careful consideration to ensure uniform and reliable reinforcement protection, if or when required.

However, it may also be that the higher driving voltage requirement could be offset by reduced corrosion rates due to the higher strength and higher resistivity of the UPC/UPBC. To ensure that ICCP systems are correctly designed further research is required to determine the inter relationship between the resistivity, corrosion rate, current distribution and output voltage requirements.

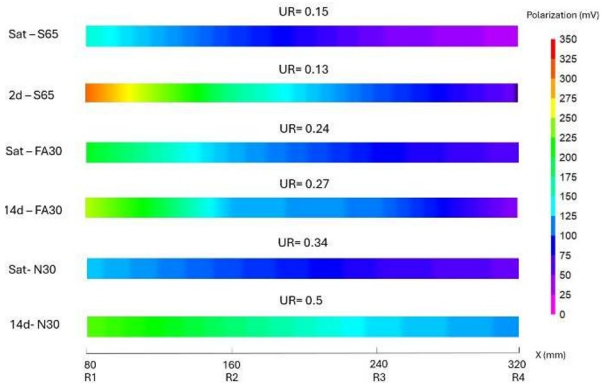

Fig. 7. Polarization distribution along bar

4 Conclusions

The following observations and conclusions can be drawn from the reported study on the influence of resistivity and distance from anode on current distribution and polarization when subject to short term application of CP.

- Mix designs were developed to provide a range of resistivities from 100 kΩ.cm (N30) to 1000 kΩ.cm (S65).
- Output voltage generally increased with increased resistivity. This is attributed to the formation of a passive layer on the steel, consumption of moisture around the steel and polarization concentration of the electrolyte.
- The driving voltage is both a function of concrete resistivity and polarization resistance of the steel.
- The polarization resistance appears to have a more significant impact at lower resistivities, while at higher resistivities, concrete resistivity becomes the dominant factor.
- At the highest resistivities the output voltage (11V) was unable to maintain a 20 mA/m^2 current.
- Saturated specimens exhibit lower polarization due the slow rate of oxygen diffusion.
- As resistivity increases the uniformity of the current distribution becomes more even in the low resistivity specimens (N30, FA30), but less even in the high resistivity specimen (S65).
- It is hypothesised that more uniform current distribution in N30 and FA30 is due to corrosion being inhibited by the drying of the concrete, coupled with the lower resistivity enabling greater throwing distance.

References

1. Sohail, M.G., et al., Durability characteristics of high and ultra-high performance concretes. Journal of Building Engineering, 2021. **33**.
2. Valcuende, M., et al., Corrosion resistance of ultra-high performance fibre-reinforced concrete. Construction and Building Materials, 2021. **306**.
3. Chess, P.M. and J. Broomfield, History and principles of cathodic protection for reinforced concrete. Cathodic Protection of Steel in Concrete and Masonry, 2nd Edition, 2014: p. 57-64.
4. Glass, G.K., W.K. Green, and J.R. Chadwick, Long term performance of cathodic protection systems on reinforced concrete structures, in UK Corrosion 91. 1991: Manchester;UK.
5. ISO:12696:2016, Cathodic protection of steel in concrete. 2016.
6. Bertolini, L., et al., Cathodic Protection of New and Old Reinforced-Concrete Structures. Corrosion Science, 1993. **35**(5-8): p. 1633-1639.
7. Hassanein, A.M., G.K. Glass, and N.R. Buenfeld, Protection current distribution in reinforced concrete cathodic protection systems. Cement & Concrete Composites, 2002. **24**(1): p. 159-167.
8. Xu, J. and W. Yao, Current distribution in reinforced concrete cathodic protection system with conductive mortar overlay anode. Construction and Building Materials, 2009. **23**(6): p. 2220-2226.
9. Goyal, A., et al., Potential and current distribution across different layers of reinforcement in reinforced concrete cathodic protection system- A numerical study. Construction and Building Materials, 2020. **262**.
10. Bruns, M. and M. Raupach, Protection of the opposite reinforcement layer of RC-structures by CP - results of numerical simulations. Materials and Corrosion-Werkstoffe Und Korrosion, 2010. **61**(6): p. 505-511.
11. AS 3972, Portland and blended cements. 2010, Australian Standard.
12. Le, H.V., et al., Electrical properties of smart ultra-high performance concrete under various temperatures, humidities, and age of concrete. Cement & Concrete Composites, 2021. **118**.
13. Raupach, M., Investigations on the influence of oxygen on corrosion of steel in concrete - Part 2. Materials and Structures, 1996. **29**(188): p. 226-232.